Available online at www.sciencedirect.com
SCIENCE DIRECT
Journal of Photochemistry and Photobiology A: Chemistry 173 (2005) 238–247
Journal of Photochemistry and Photobiology A:Chemistry
www.elsevier.com/locate/jphotochem

Complexes of dihexyl 2,6-naphthalenedicarboxylate with α- and β-cyclodextrins: Fluorescence and molecular modelling

Isabel Pastor, Antonio Di Marino, Francisco Mendicuti *

Departamento de Química Física, Universidad de Alcalá, 28871 Alcalá de Henares, Madrid, Spain

Available online 17 May 2005

Abstract

Fluorescence techniques and molecular mechanics (MM) were used to study the inclusion complexes of dihexyl 2,6-naphthalenedicarboxylate (DHN) with α- and β-cyclodextrins (CDs). Stoichiometries, formation constants and the changes of enthalpy and entropy upon inclusion were also obtained by measuring the variation, with CD concentration and temperature, of the relative intensity of two peaks shown in all steady-state emission spectra. Results agree with the formation of 1:1 αCD:DHN and 2:1 βCD:DHN stoichiometry complexes. MM calculations in the presence of water were employed to study the formation of different stoichiometry complexes of DHN with both α- and βCDs. For the most stable structures of 1:1 complexes a large portion of DHN is exposed to the solvent making it possible for another CD to approach. Driving forces for 2:1 inclusion processes may be dominated by non-bonded van der Waals CD–DHN interactions. However, due to the different structures of the 2:1 complexes, an important electrostatic interaction appears between both βCDs in the βCD_2:DHN complex. This interaction does not exist between αCDs in the αCD_2:DHN complex. Most of this contribution is due to the intermolecular hydrogen bonding formation between secondary hydroxyl groups of both βCDs. The average of the lifetime measurements $\langle\tau\rangle$ with the CD added also supports the formation of such stoichiometry complexes.

Keywords: Cyclodextrins; Inclusion complex; Fluorescence; Molecular mechanics; Dihexyl 2,6-naphthalenedicarboxylate

1. Introduction

Cyclodextrins (CDs) are macrocyclic torus-shaped molecules formed by D-(+)-glucopyranose units. CD size and shape are correlated to the type and number of (1,4) linkages between those units. The most well-known CDs, named α-, β- and γCDs, are those with 6, 7 and 8 of those units respectively. CDs are suitable to form inclusion complexes with low molecular weight compounds and polymers giving interesting supramolecular assemblies [1–4]. Size, shape and polarity of the guest molecule relative to the CD low polar inner cavity are critical parameters for the complexation. Fluorescence spectroscopy [5–21] is useful for solving the thermodynamics accompanying the inclusion for guests containing fluorophore groups. Molecular modelling [22,23] can also provide information about the structure of the complexes and about their driving forces.

We have been using the combination of fluorescence and molecular modelling to study the inclusion phenomena of small molecules with CDs [16–21]. One of our studies was focused on the inclusion of diesters derived from the 2,6-naphthalenedicarboxylic acid, *S*-OOC-$C_{10}H_6$COO-*S*, with α- and βCDs, where *S* = CH_3- [19] or CH_3-CH_2-groups [20]. The compounds are named dimethyl 2,6-naphthalenedicarboxylate (DMN) and diethyl 2,6-naphthalenedicarboxylate (DEN) respectively. DMN and DEN emission spectra showed two peaks, like many other naphthalene derivatives [16–18,21], whose ratio of intensities was very sensitive to medium polarity. Thermodynamics of complexation was studied through the changes of this ratio with the CD concentration and temperature. DMN form complexes of stoichiometries 2:1 and 1:1 with α and βCD [19] respectively whereas DEN prefers 2:1 stoichiometries with both hosts [20]. The estimated association constants at 25 °C for DMN complexes were relatively large, $\sim 8.0 \times 10^5\ M^{-2}$ and $\sim 1.3 \times 10^3\ M^{-1}$ for αCD_2:DMN and βCD:DMN respectively. The stability of the βCD_2:DEN

* Corresponding author. Tel.: +34 91 8854672; fax: +34 91 8854763.
E-mail address: francisco.mendicuti@uah.es (F. Mendicuti).

1010-6030/$ – see front matter © 2005 Elsevier B.V. All rights reserved.
doi:10.1016/j.jphotochem.2005.04.003

complex ($\sim 2.7 \times 10^4\ M^{-2}$) is slightly larger than that of αCD_2:DEN ($\sim 1.3 \times 10^4\ M^{-2}$). Both 2:1 complexes however exhibit smaller stability than the αCD_2:DMN complex. Molecular mechanics, in agreement with thermodynamic parameters changes, demonstrates that the complexes were mainly stabilized by van der Waals interactions existing between host and guest. Nevertheless, CDs approach to distances where electrostatic non-bonded interactions appear between them for αCD_2:DMN and βCD_2:DEN complexes. These interactions hardly exist in the αCD_2:DEN complex. This contribution was attributed to the intermolecular hydrogen bonding formation between secondary hydroxyl groups of both CDs.

The purpose of the present work is to study the complexation of the dihexyl 2,6-naphthalenedicarboxylate, another diester guest where $S = CH_3\text{-}(CH_2)_5$ – is a longer chain capable of exhibiting rather coiled conformations, with α- and βCDs from the experimental and theoretical points of view. Association constants and enthalpy and entropy changes were obtained. Results were rationalized by emulation of the complexation processes using Molecular mechanics and they were compared with those obtained for DMN and DEN inclusion processes with both CDs.

2. Details and methods

2.1. Materials

The dihexyl 2,6-naphthalenedicarboxylate (DHN) guest, depicted in Fig. 1, was synthesized by reaction of 2,6-naphthalenedicarboxylic acid chloride with *n*-hexanol in presence of triethyl amine in a manner similar to that described previously for the analogous diethyl 2,6-naphthalenedicarboxylate (DEN) diesters [20]. Details for the synthesis of similar compounds were previously reported [24]. Purification was achieved by recrystallization (3×) from the chloroform solutions by adding a slight amount of methanol. Characterization was mainly done by NMR. The αCD (Aldrich) was used as received and the βCD (Aldrich) was recrystallized (2×) from water. Water content of ∼10% and 6% for the α- and βCD respectively were obtained by thermo gravimetric analysis (TGA). DHN solutions in the presence of CDs were prepared by weight, from a double-filtered (Millipore, 0.45 μm Ø cellulose filters) aqueous DHN saturated solution ($<10^{-6}$ M). Concentrations of α- and βCD ranged from 0 to 1.20×10^{-2} and 1.29×10^{-2} M respectively, while the guest concentration was maintained constant in all experiments. All solutions were stirred for about 2 days before measuring.

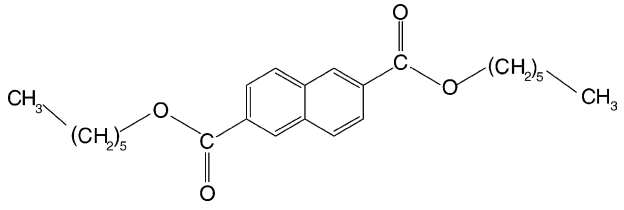

Fig. 1. Structure of the DHN guest.

2.2. Apparatus

Steady-state and time resolved fluorescence measurements were performed by using an SLM 8100 AMINCO Spectrofluorimeter and a time-correlated single-photon-counting FL900 Edinburgh Instruments Spectrometer equipped with a lamp filled with N_2. Characteristics of both instruments and measurement conditions were similar to those described previously [20]. Emission spectra were obtained upon 294 nm as excitation wavelength. Decay profiles were collected by exciting at 296 nm, one of the peaks of the spectral output of the N_2 lamp, by selecting the emission at 385 nm. Measurements of different solutions were performed at 10 °C intervals in the 5–45 °C temperature range (Techne RB-5, TE-8A).

2.3. Theoretical methods

The calculations were performed with Sybyl 6.9 [25] and the Tripos Force Field [26]. Bond stretching, angle bending, torsion, van der Waals, electrostatics, and out-of-plane energies contributed to the total potential energy. As in previous calculations [19,20] a relative permittivity of 3.5 in vacuum and a lineal function of the distance in the presence of water were used. DHN and water molecule charges were obtained by MOPAC [27]. CDs and water charges were the same as used previously [17–20]. Non-bonded cut-off distances were set at 8 Å. Minimization of the of the system was performed by the simplex algorithm and the conjugate gradient was used as a termination method (gradients 0.2 and 3.0 kcal mol^{-1} $Å^{-1}$ in vacuum and in water respectively) [28]. Water addition was achieved by the Molecular Silverware (MS) [29] algorithm. Periodic Boundary Conditions (PBC) were employed.

Binding energy or any of its contributions, E_{bin} for a complex, were obtained as the difference between the potential energy of the complex and the sum of the potential energies of the isolated DHN and CD. The strain energy of CDs is the sum of torsional, stretching and bending energies. Some relaxed criteria were used for the hydrogen bond (O–H···O′) formation: the H···O′ distance and the O′–H–O angle are in the 0.8–2.8 Å range and larger than 120° respectively.

3. Results and discussion

3.1. Fluorescence measurements

Fig. 2 depicts the uncorrected emission spectra at 25 °C of DHN and DHN/CD water solutions at different

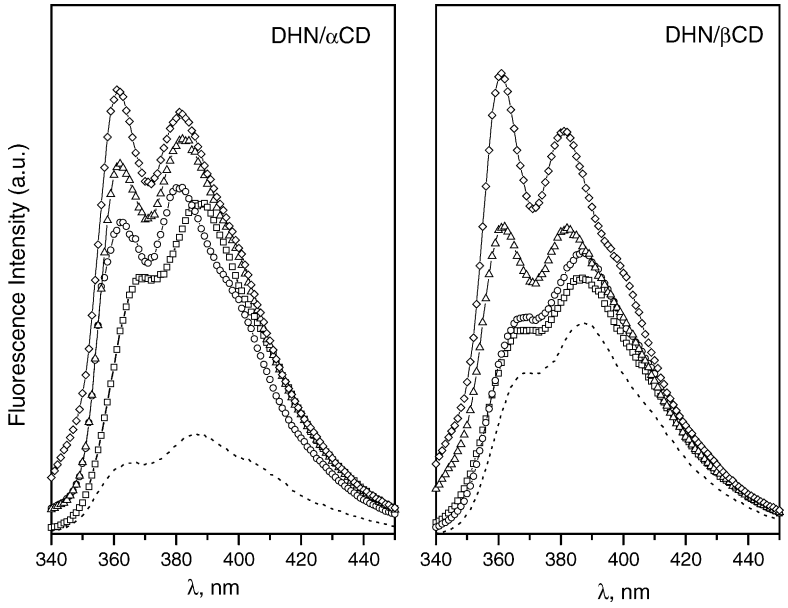

Fig. 2. Uncorrected emission spectra of DHN aerated aqueous solutions at five CD concentrations and at 25 °C upon λ_{exc} = 294 nm. (a) [αCD] = 0 (dashed line), 0.58 (□), 1.9 (◯), 9.0 (△) and 12.0 (◊); (b) [βCD] = 0 (dashed line), 0.58 (□), 2.6 (◯), 9.0 (△) and 12.9 (◊); The [DHN] was held constant (<10^{-6} M).

concentrations of αCD or βCD. Spectra look like those reported for DMN [19] and DEN [20] water solutions with both CDs. They show even analogous characteristics: (a) no isoemissive points are distinguished; (b) the fluorescence intensity (area under emission spectrum) of the DHN water solution substantially increases in the presence of αCD; this relative increase, however, is smaller when βCD is added; in general an increase of fluorescence intensity for both DHN/αCD and DHN/βCD solutions with CD concentration is observed; this increase, however, is slightly larger for the latter; (c) two overlapping bands, whose maxima in the absence of CD are placed at 368 and 386 nm, that are shifted a few nanometers toward the high energy region of the spectrum upon the addition of CD are observed. The main feature, however, is the change that takes place in the relative intensity of both bands with [CD]. The low energy band intensity decreases and the high one increases with [CD].

Quantitatively this change can be measured by the ratio *R* of intensities of the low and high energy peaks ($I_{\sim 386\,nm}/I_{\sim 368\,nm}$). Fig. 3 depicts the variation of *R* with [CD] for the DHN/CD solutions at different temperatures. *R* monotonically decreases upon addition of CD. This decrease with [CD], however, depends on the host. Quantitatively this decrease is always larger at the lowest temperatures. The lowest value of *R* obtained for a given [CD] at the lowest temperature is related to the larger amount of DHN that is complexed at this temperature, suggesting a larger association constant and therefore a negative enthalpy change accompanying complexation. Similar effects were observed with DMN, DEN and other naphthalene derivative guests [17–21]. The change in *R* is usually associated with the decrease in polarity of the medium surrounding the chromophore guest during complexation.

3.2. Fluorescence intensity decays

In spite of the low fluorescence signals, the decay profile for a DHN water solution in absence of CD can be fitted to

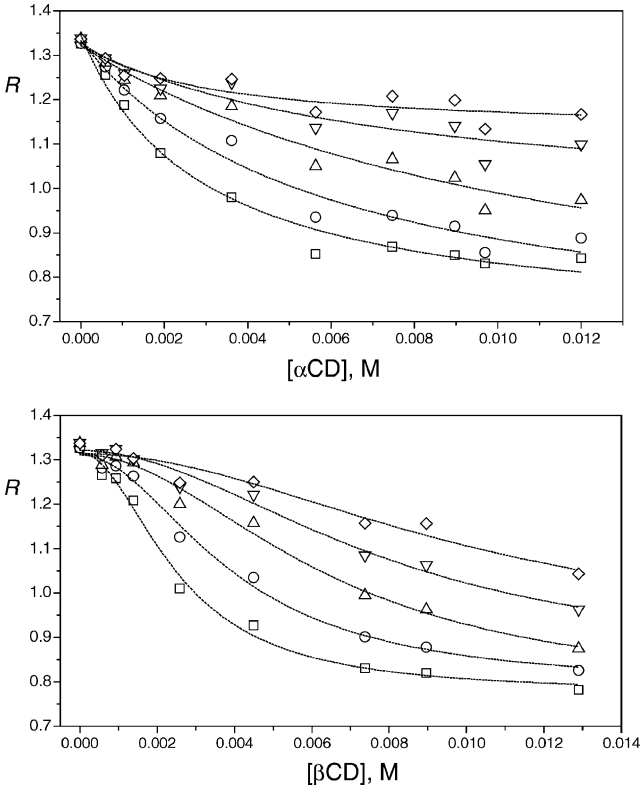

Fig. 3. Variation of *R* with [αCD] (top) and [βCD] (bottom) at 5 (□); 15 (◯); 25 (△); 35 (▽); 45 °C (◊). Curves were obtained by adjusting the experimental data by using Eq. (7).

single exponential decay functions, while those containing CD can be reasonably adjusted to double exponential decay functions ($\chi^2 \approx 1.1$–1.4). The single lifetime component, τ_0, in the absence of CD is ascribed to the free DHN guest. τ_0 decreases as the temperature increases, showing values of 14.4, 13.4, 12.4, 11.3 and 10.4 ns as the temperature increases from 5 to 45 °C at 10° intervals respectively. As previously [20], the analysis of the profile decays for DHN/CD solutions was carried out by fixing one component τ_1 to τ_0. Then a second component τ_2 was obtained from the iterative reconvolution analysis [30]. τ_2 was always longer than τ_1 but it decreased with temperature. Thus, τ_2 values were 22.4 ± 1.8, 21.2 ± 2.2, 19.4 ± 1.8, 18.3 ± 1.2 and 16.8 ± 0.9 ns as the temperature increased from 5 to 45 °C respectively. This component could be associated to the complexed form.

The fractional contribution f_i of each decay time to the steady-state intensity which represents the fraction of total fluorescence intensity due to component i at the wavelength of observation is given by [31]:

$$f_i = \frac{A_i \tau_i}{\sum_i A_i \tau_i} = \frac{I_i}{\sum_i I_i} \quad (1)$$

where A_i is the pre-exponential factor of the component with a lifetime τ_i of the multiexponential function intensity decay. On the other hand, the intensity weighted average lifetime $\langle\tau\rangle$ for a double-exponential decay can be obtained as

$$\langle\tau\rangle = f_1\tau_1 + f_2\tau_2 \quad (2)$$

Values of f_2 (subscript 2 is attributed to the complexed guest) increase upon CD addition while f_1 decreases. Fig. 4 depicts the variation of $\langle\tau\rangle$ with [CD] for DHN and α- or βCD water solutions at different temperatures. At each temperature, from the initial value in the absence of CD (τ_0), $\langle\tau\rangle$ increases monotonically with CD concentration. This increase is due to the larger fraction of the complexed form, where the guest is presumably located in a higher microviscosity medium with a larger lifetime component than the free DHN guest. $\langle\tau\rangle$ also decreases with temperature. This is probably due to the decrease in the amount of the complexed form (if $\Delta H < 0$) and the temperature effect on both lifetime components of the free and complexed guest. While R mainly depends on medium polarity, $\langle\tau\rangle$ is mainly dependent on the medium microviscosity surrounding the guest. The inclusion process in a relatively hydrophobic CD cavity should be accompanied by a decrease of medium polarity (R) and an increase of microviscosity ($\langle\tau\rangle$).

3.3. Binding constants

For a $CD_n : G$ complex, with stoichiometry 1:n, whose global equilibrium can be written as

$$n\,CD + G \rightleftharpoons CD_n : G \quad (3)$$

assuming $[CD]_0 \approx [CD]$ and one unique complex $CD_n : G$ is supposed to exist, the molar fraction of complexed G, x_2 ($\neq f_2$), for equilibrium (3) can be written as

$$x_2 = \frac{[CD_n : G]}{[G]_0} = \frac{K[CD]_0^n}{1 + K[CD]_0^n} \quad (4)$$

where K is the association constant written as

$$K = \frac{[G : CD_n]}{[G][CD]^n} \quad (5)$$

The molar fraction x_2 can be evaluated from the steady-state measurement through the parameter R as it is related to the polarity around the guest as

$$x_2 = \frac{R_0 - R}{R_0 - R_\infty} \quad (6)$$

where the subscripts 0 and ∞ are the values at $[CD]_0 = 0$, for free DHN and at $[CD]_0 = \infty$ for the complex. From Eqs. (5) and (6) the following be obtained

$$R = \frac{R_0 + R_\infty K[CD]_0^n}{1 + K[CD]_0^n} \quad (7)$$

Curves depicted in Fig. 3 for DHN/αCD and DHN/βCD systems are the results of the non-linear regression analysis [32] derived from Eq. (7). Adjustments indicate stoichiometries 1:1 and 2:1 for DHN complexes with α- and βCDs respectively. Table 1 collects the association constants obtained from these adjustments, as well as the values for R_0 and R_∞.

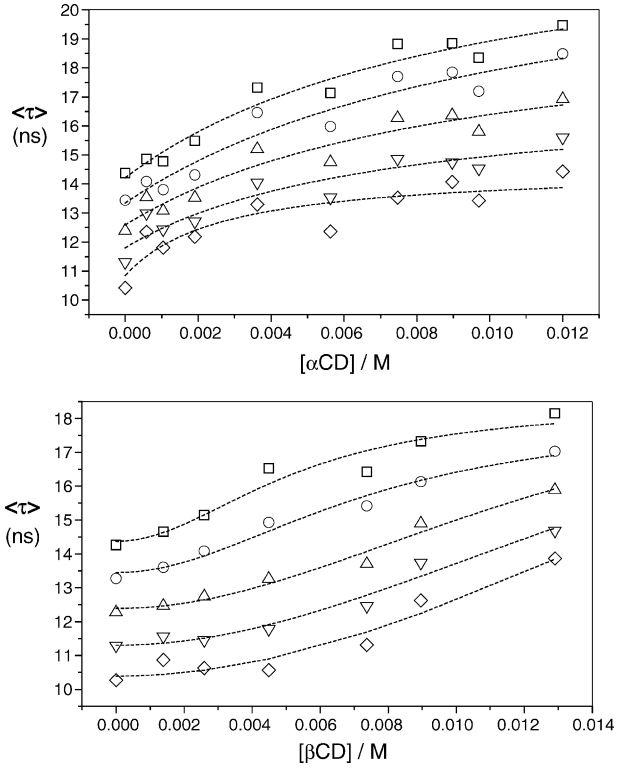

Fig. 4. Variation of the average of lifetime $\langle\tau\rangle$ with [αCD] (top) and [βCD] (bottom) at 5 (□); 15 (◯); 25 (△); 35 (▽); 45 °C (◊). Curves were obtained by adjusting the experimental data by using Eq. (10) and the association constants obtained from steady-state measurements.

Table 1
Association constants K, R_0 (τ_0) and R_∞(τ_∞), as well as, their absolute errors for αCD:DHN and βCD_2:DHN at five temperatures, determined from measurements of R by using nonlinear regression fits from Eq. (7)

T (°C)	$K \times 10^{-2}$ (M^{-1})	R_0 (τ_0)	R_∞ (τ_∞)	d/e
αCD:DHN				
5	3.5 ± 0.8	1.346 ± 0.025 (14.2 ± 0.4)	0.683 ± 0.042 (23.5 ± 2.8)	(0.30 ± 0.20)
15	2.3 ± 0.7	1.340 ± 0.023 (13.3 ± 0.4)	0.682 ± 0.068 (23.0 ± 4.1)	(0.38 ± 0.31)
25	1.6 ± 0.7	1.332 ± 0.022 (12.5 ± 0.4)	0.776±0.104 (19.9 ± 2.8)	(0.66 ± 0.53)
35	1.3 ± 1.2	1.329 ± 0.023 (11.8 ± 0.4)	0.950 ± 0.154 (17.2 ± 2.3)	(1.06 ± 1.00)
45	3.4 ± 2.5	1.256 ± 0.005 (10.8 ± 0.5)	1.127 ± 0.040 (14.5 ± 0.9)	(1.11 ± 1.01)
T (°C)	$K \times 10^{-4}$ (M^{-2})	R_0 (τ_0)	R_∞ (τ_∞)	d/e
βCD_2:DHN				
5	15.7 ± 2.6	1.316 ± 0.014 (14.4 ± 0.3)	0.774 ± 0.016 (18.4 ± 0.7)	(0.22 ± 0.14)
15	6.5 ± 1.1	1.311 ± 0.017 (13.4 ± 0.2)	0.798 ± 0.020 (18.1 ± 0.6)	(0.27 ± 0.10)
25	2.4 ± 0.6	1.312 ± 0.012 (12.4 ± 0.2)	0.773 ± 0.046 (21.3 ± 6.2)	(0.22 ± 0.15)
35	1.6 ± 0.5	1.320 ± 0.010 (11.3 ± 0.2)	0.836 ± 0.058 (21.3 ± 6.2)	(0.20 ± 0.18)
45	0.9 ± 0.5	1.314 ± 0.011 (10.4 ± 0.2)	0.884 ± 0.116 (28.6 ± 3.3)	(0.15 ± 0.33)

In parentheses are the values for τ_0, τ_∞ and d/e by using nonlinear regression fits from Eq. (10) by fixing K values to the ones obtained from steady-state measurements.

The low fluorescence signal, due to the low DHN water solubility, contributes to the relatively large uncertainties of the results. R_0 values, which are very similar for both systems, seem not to depend much on temperature. The values of R_∞, which is a measure of the polarity surrounding the complexed guest, denote that, at 25 °C, for both complexes DHN guest are located in a similar polarity environment. Stoichiometries of the DHN complexes formed differ from those studied by us with other guest diesters, DMN and DEN, whose substituents *S* are shorter, methyl or ethyl groups respectively. DMN complexes with α- and βCD giving 2:1 and 1:1 CD:DMN stoichiometries respectively, whereas DEN always prefers 2:1 CD:DEN stoichiometries.

The association constants obtained from steady-state measurements were relatively low, 159 M^{-1} and 24500 M^{-2} for αCD:DHN and βCD_2:DHN at 25 °C respectively. The constant for αCD:CHN is in the same order as other 1:1 complexes of naphthalene derivatives with αCD, like 2-methyl naphthoate (200 M^{-1}), and always smaller than their corresponding complexes 1:1 with βCD (2000 M^{-1}) [33]. The association constant for βCD_2:DHN is similar to the one for βCD_2:DEN (2.7×10^4 M^{-2}) and smaller than that for αCD_2:DMN (81.9×10^4 M^{-2}) at the same temperature reported by us [19,20]. These results indicate that at 25 °C approximately 65% of DHN is complexed with one αCD and that 78% is with two βCDs when CD is added up to approximately the maximum concentration of CD reached in our experiments, 0.012 M. At this CD concentration almost all DMN (99.1%) was complexed with a couple of αCDs.

On the other hand we can express the steady-state fluorescence intensity at a given wavelength of the guest at any [CD] as [9]:

$$I_2 = kdx_2[\mathrm{G}]_0 \tag{8}$$

where x_2 was defined in Eq. (4), and the total intensity as

$$I = k\{e(1 - x_2)[\mathrm{G}]_0 + dx_2[G]_0\} \tag{9}$$

where $[\mathrm{G}]_0$ (= [G] + [CD_n : G]) is the initial concentration of the guest, k a constant which depends on instrumental conditions, e and d are the factors for the quantum yield change of the free and complexed guest respectively in the presence of CD, relative to the quantum yield of the isolated (in the absence of CD) free guest due to the interactions with the new components of the system. But the d factor also comprises the variation in quantum yield that takes place when the free guest complexes [9].

From Eqs. (1) and (2) the following equation is derived by substituting the values of Eqs. (4), (5), (8) and (9):

$$\langle\tau\rangle = \frac{\tau_0 + \tau_\infty(d/e)K[\mathrm{CD}]_0^n}{1 + (d/e)K[\mathrm{CD}]_0^n} \tag{10}$$

Fig. 4 also shows the results of the nonlinear adjustment derived from Eq. (10) that reproduces the results of association constants obtained by the steady-state method. Curves seem to reasonably fit the experimental results and they also reproduce the 1:1 and 2:1 stoichiometries, which are characterized by the typical curve shape at the lowest [CD]. Values of τ_0, τ_∞ and d/e parameters, collected in Table 1, are subject to large uncertainties due to intrinsic reasons of the method. These results, however, seem reasonable. Values of d/e increase with temperature when DHN complexes with αCD whereas they are almost constant for the DHN/βCD system. It is difficult to independently relate this ratio with the quantum yield changes of the free (e) and the complexed (d) guest upon complexation. τ_0 obtained from the fit are very similar for both systems and to the experimental values for free DHN in the absence of CD, τ_0 at each temperature. On the contrary, the values of τ_∞, which are obviously larger than τ_0, also depend on the CD used.

3.4. Variation of enthalpy and entropy

ΔH° and ΔS° were obtained from van't Hoff plots, using the association constants collected in Table 1. Fig. 5

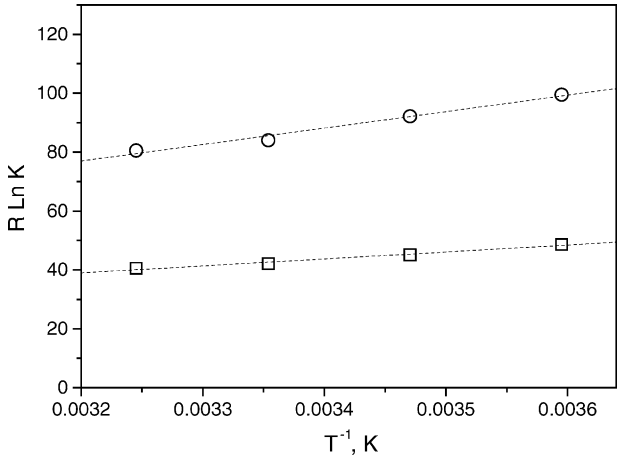

Fig. 5. Van't Hoff plots for the formation of αCD:DHN (□) and βCD_2:DHN (◯). Values of K at 45 °C were excluded due to the large uncertainties.

depicts these plots for both αCD:DHN and βCD_2:DHN complexes obtained from steady-state. They are reasonably linear ($r = 0.992$). Table 2 shows the enthalpic and the entropic terms including those for DMN [19] and DEN [20] complexation with both CDs. Both DHN inclusion processes are enthalpically governed with an unfavorable entropic term. ΔH° for the formation of 1:1 αCD:DHN (−23.6 kJ/mol) is similar to the values obtained for the 1:1 complexation of 2-methyl naphthoate with αCD reported by us [16], and always more negative than the values obtained for the 1:1 complexation with βCD [16,21]. This negative sign is typical of large guests trying to penetrate into a relatively small cavity, where van der Waals host–guest interactions are important. The entropic term reveals that ΔS° for 1:1 αCD:DHN is also negative (−36.6 J/kmol). Something similar occurred with 9-methyl anthroate and 2-methyl pyrenoate when they complexed with βCD [18]. Complexation of both guests also gave negative entropy changes. Part of these guests were exposed to the solvent in the complexes, diminishing the positive entropy contribution due to the breaking of the solvent shell around the guests during the complex formation. ΔH° for the 2:1 βCD:DHN complex is also negative but shows larger absolute values than the ones obtained for the 1:1 complexes with βCD. These values are quantitatively similar to the ones obtained for 2:1 complexes of DEN with both CDs and smaller than the value with the 2:1 complex of DMN with the smallest αCD. These results were again typical of hydrophobic guests whose complexation is driven by van der Waals interactions and/or hydrogen bonding or any other attractive interaction which makes enthalpy decrease during the process. ΔS° is also negative (−102.3 J/kmol) for 2:1 βCD:DHN. Negative entropy changes were also found for 2:1 complexes of DMN with αCD and DEN with α- and βCDs. These negative values were explained as a consequence of the fact that the guest is almost totally immobilized inside the cavity of both CDs.

Table 2
Values of the enthalpy (ΔH°) and entropy term ($-T\Delta S^\circ$) for different complexes

Complex	ΔH° (kJ mol^{-1})	$-T\Delta S^\circ$ (kJ K^{-1} mol^{-1})
αCD_2:DMN[a]	−100.4 ± 1.6	+66.5 ± 1.5
βCD:DMN[a]	−13.4 ± 0.3	−4.4 ± 0.3
αCD_2:DEN[b]	−45.3 ± 4.1	+20.2 ± 4.2
βCD_2:DEN[b]	−46.6 ± 5.0	+20.4 ± 4.9
αCD:DHN[c]	−23.6 ± 2.1	+10.9 ± 2.2
βCD_2:DHN[c]	−56.0 ± 5.2	+30.5 ± 5.2

[a] From Ref. [19].
[b] From Ref. [20].
[c] Removing the data at 45 °C whose K values have large errors.

3.5. Molecular mechanics

Schemes of 1:1 and 2:1 inclusion strategies are depicted in Fig. 6. Details of these processes were similar to the ones described previously [19,20]. CDs were initially in the non-distorted form. From the analysis of the 5000 structures obtained from the 1 ns MD simulation in the vacuum, whose characteristics were described previously [20], two guest conformations were initially selected as starting geometries for the emulation of the 1:1 complexation. One of them, which is quite coiled, depicted on top of Fig. 6, corresponds to the lowest energy conformation (13.7 kcal mol^{-1}) and the other one, shown on the bottom, to the conformation with lowest energy (16.4 kcal mol^{-1}) which is fairly extended. In the remainder of this manuscript such conformations will be named *C* and *E* respectively. Three parameters define the relative host–guest approaching: θ, the inclusion angle (plane angle between *yz* and the DHN guest naphthalene ring); δ, the $oo'C_9$ angle and the oo' distance along *y* coordinate. For the 1:1 complexation process the DHN was moved step by step along this coordinate for a previously fixed pair of θ and δ parameters. Then each structure generated was solvated and minimized. θ and δ optimized pairs were obtained by critical inspection of the three-dimensional $E_{bin} - \theta - \delta$ maps obtained by analysis of the structures generated in the vacuum by incrementally scanning such parameters at different CD-host distances. Results of this inspection indicate that the most favorable δ and θ pairs were ∼90°, 40° (60°, 5°) and 90°, 55° (55°, 5°), when *C* (*E*) approached the α- and βCDs respectively. The 2:1 complexation process, however, was emulated starting from the 1:1 stoichiometry structure of minimum binding energy (MBE) by approaching a second CD, as shown at the bottom of Fig. 6. In a similar manner, each structure generated was solvated and minimized. The oo'' distance along the *y* axis defines the CD separation. The association angle θ' initially at 0° was measured by the dihedral $O(4)$–o–o''–$O'(4)$ angle.

Fig. 7 depicts binding energies obtained upon *C* (*E*) approaching each CD from $y = +16$ (+20) to $y = -4$ (−2) at 0.5 intervals, measured in Å. This figure shows the inclusion process with αCD (top) and βCD (bottom). Binding energy seems to decrease during the approaching. Nevertheless, the presence of some unfavorable energy barriers means that the guest should surmount them in order to penetrate into the cavity. These barriers are obviously larger for

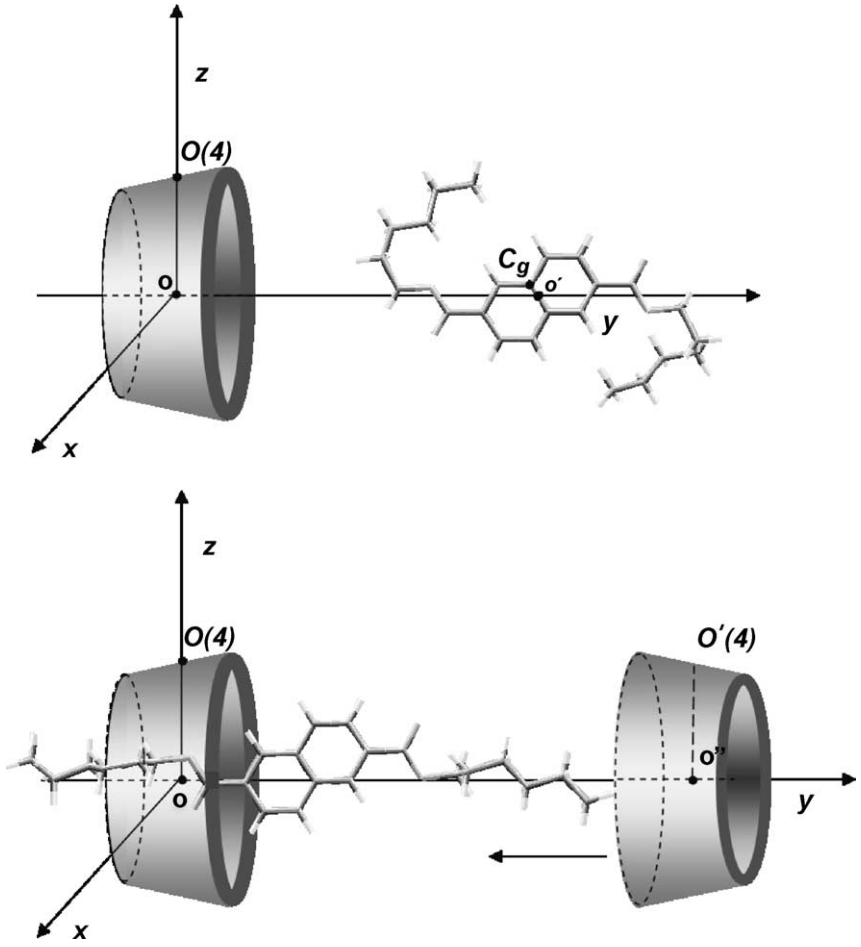

Fig. 6. Scheme for the 1:1 (top) and 2:1 (bottom) formation of host-DHN complexes.

the complexation with αCD. Surmounting some small barriers during the approach of DHN to βCD, the structures of MBE named 1Cβ and 1Eβ, shown at the bottom of Fig. 7, are reached at y(Å) = +1.2 (+4.9) where $\delta = 56.2^\circ$ (56.5°) and $\theta = 54.9^\circ$ (1.3°) when C (E) approaches the host. At this point E_{binding} is −40.4 kJ/mol (−55.2 kJ/mol). Even if part of the guest penetrates into the CD cavity, as depicted, a significant portion of it is also left out. Binding energy for the complexation of C with αCD shows a large positive unfavorable energy gap for $y < +10.7$ (Å). This makes 1Cα, with $y = +10.7$ (Å), $\delta = 6.8^\circ$, $\theta = 51.4^\circ$ and $E_{\text{bin}} = -18.3$ kJ/mol the most feasible structure for this complex. Only a very small part of C is inside the cavity. The inclusion of a more extended DHN conformation (E) is also accompanied by a relatively large gap which is centered around $y = +12$ (Å) with $E_{\text{bin}} > 0$. Assuming that this barrier is surmounted during complexation, the most feasible structure would be 2Eα with y(Å) = +4.6 where $\delta = 59.0^\circ$ and $\theta = 10.3^\circ$. If it is not the geometry of the complex, 1Eα, should be similar to 1Cα where almost all DHN is outside the αCD cavity.

More than 90% of the stabilization of 1:1 complexes at the MBE comes from van der Waals non-bonded interactions, the remaining part is due to electrostatic ones. The CD:DHN formation with any of the CDs when C approaches is accompanied by an increase of total potential energy. When E approaches, however, a slight decrease in such energy takes place. This is mainly due to the increase in both the CD macroring and the DHN strains.

As was pointed out earlier, an important characteristic of the geometry for 1:1 complexes is that a relatively large portion of the guest is outside the CD cavity. This suggests the possibility of the approaching of a second CD to the previously formed 1:1 complex. The theoretical emulation of the process has already been described.

The left panel of Fig. 8 shows the change in the binding energy between guest and CD hosts, E_{bin} [G − (CD + CD′)] as a function of the oo'' distance during the approaching of a second CD′ to the of MBE structure of the (1:1) CD:G complex. Binding energies when E complexes with both CDs decrease with the CD separation reaching a minimum value. The y coordinate of o'' and o' center of masses for the structures of minimum E_{bin} (MBE′) when E complexes are accomplished at +8.1 and +4.1 (Å) for αCD_2:DHN (−115.2 kJ mol^{-1}) and of +8.0 and +4.7 (Å) for βCD_2:DHN (−114.2 kJ mol^{-1}). Most of the attractive E_{bin} [G − (CD + CD′)] interaction at the MBE′ is due to van der Waals contribution (>99%). The

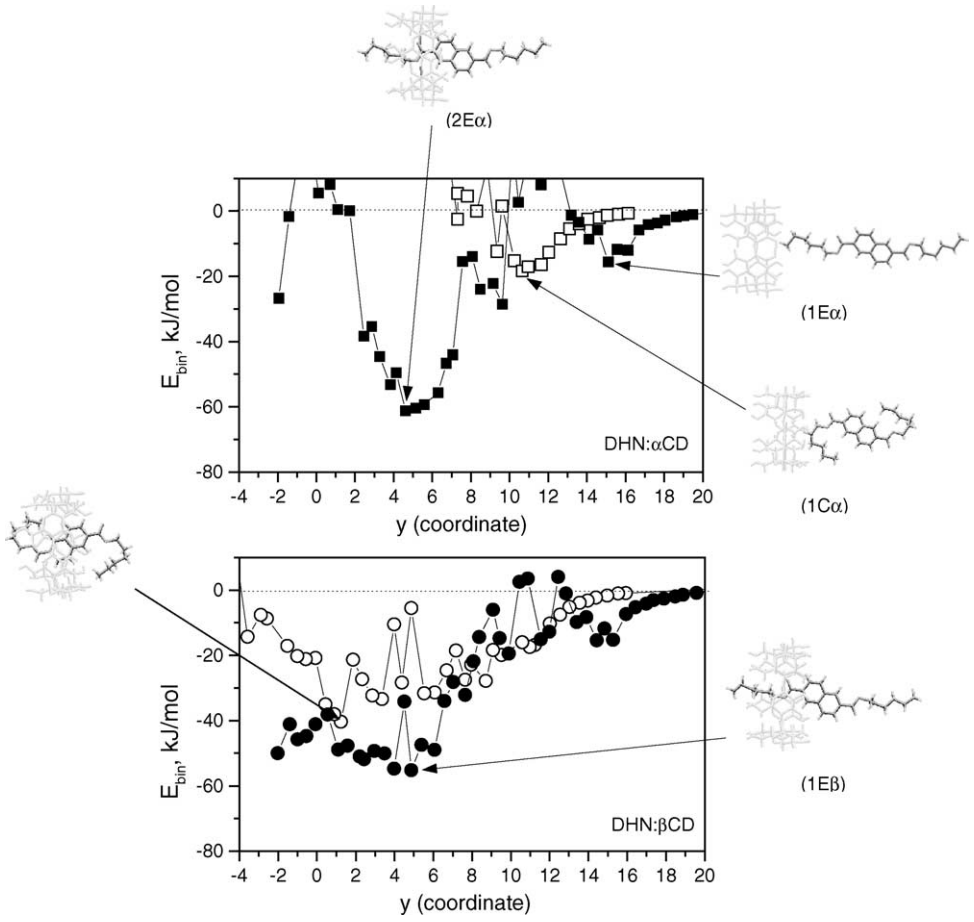

Fig. 7. Binding energies as a function of *y* coordinate (Å) for *C* (open symbols) and *E* (filled symbols) conformations of DHN guest when complexed with αCD (squares) and βCD (circles). Superimposed are depicted some 1:1 stoichiometry structures (removing water molecules) that correspond to minima binding energies.

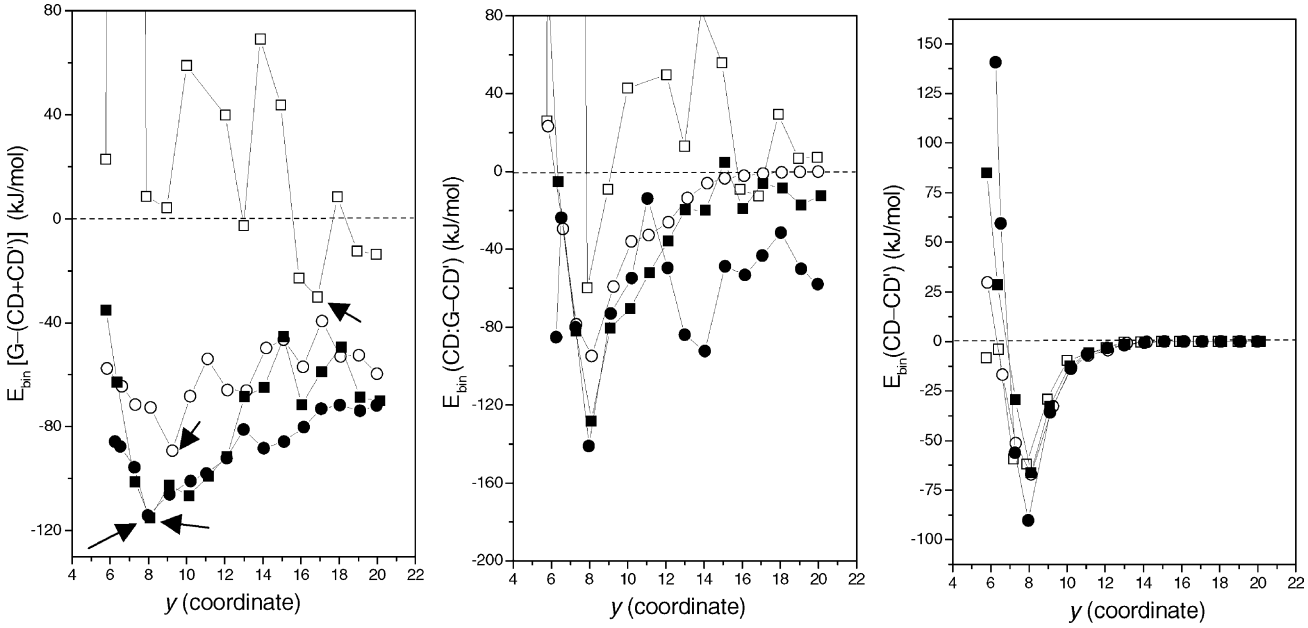

Fig. 8. $E_{bin}[G - (CD + CD')]$ (left), $E_{bin}[(CD:G) - CD']$ (center) and $E_{bin}[CD - CD']$ (right) as a function of the distance between αCDs (squares) or βCDs (circles) hosts along the *y* coordinate, for the formation of 2:1 complexes with *C* (open symbols) and *E* (filled symbols) conformation of DHN.

central and right panels of Fig. 8 also depict the interaction energy E_{bin}[(CD:G) − CD′)] and E_{bin}[CD − CD′] versus oo'' distance respectively. At the MBE′, E_{bin}[(CD:G) − CD′)] also shows a global minimum that denotes the feasibility of the formation of 2:1 complexes with both CDs when the conformation is relatively extended (*E*). For the structures of MBE′ the centers of both CDs are separated by ∼8 Å. At this distance, according to the right panel, a strong attractive interaction that contributes to stabilizing the 2:1 complexes occurs between both CDs. This stabilization arises almost equally from electrostatics and van der Waals non-bonded interactions. This distance (∼8 Å) is also appropriate for the formation of intermolecular hydrogen bonds (HBs) between both CDs. According to the criteria of HB formation, the structures of MBE′ when *E* complexes with αCD (βCD) contains 11 (12) intra- and 10 (13) intermolecular HBs respectively.

The situation for *C* complexing both CDs is somewhat different. E_{bin} [G − (CD + CD′)] increases when *C* complexes with αCD and it decreases when it does with βCD. MBE′ structures are reached at o'' and o' *y* coordinates of 16.9 and +10.5 (Å) for αCD_2:DHN ($-30.2\,kJ\,mol^{-1}$) and +9.3 and +1.2 (Å) ($-89.3\,kJ\,mol^{-1}$) for βCD_2:DHN. van der Waals contribution to E_{bin} [G − (CD + CD′)] is no larger than 80%. For βCD_2:DHN the distance between CDs is only slightly large than 8 Å and it therefore behaves in a way similar to the *E* complexation with both CDs. The MBE′ structure contains 12 intra- and 1 intermolecular HBs respectively. The cavity is large enough to accommodate a coiled DHN guest. However, E_{bin}[G − (CD + CD′)] interaction, as well as the non-bonded E_{bin}[(CD:G) − CD′)] one when *C* complexes with αCD, as Fig. 8 shows, are much less favorable. The interaction energy between both CDs also shows this characteristic; the distance between αCDs is large enough not to allow any CD interactions, thus avoiding the formation of intermolecular HBs that would favor the formation of a 2:1 stoichiometry complex.

According to the results the coiled conformations of DHN, which are probably most favored, are not capable of forming complexes with two αCDs. However, both coiled and extended conformations could reasonably form 2:1 stoichiometry complexes with βCDs. This may be the reason for the experimental formation of 1:1 αCD:DHN and 2:1 βCD:DHN complexes. Fig. 9 depicts the MBE′ structure for 2:1 βCD:DHN complex when the *E* and *C* conformations of DHN complexes with two βCD, showing intra- and intermolecular HBs between both CDs.

The stoichiometry of both complexes and subsequently the geometry of them could account for the negative sign of entropy variation during complexation. The single αCD do not shield the DHN from the solvent in the 1:1 complex. As a consequence the important positive contribution is diminished due to the fact that most of the ordered water shell around the guest is unaltered during the complexation. The unfavorable entropy term for βCD_2:DHN complexation may, however, be attributed to the loss of rotational and translational freedom degrees during the process of a guest almost immobilized inside the cavity of both CDs since both guest and host molecules have lost the ordered water molecules which solvated them during complexation.

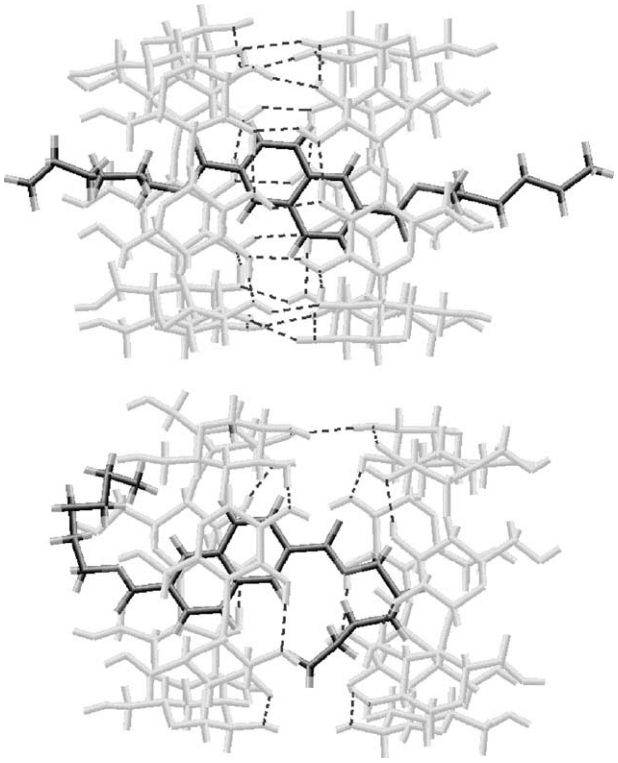

Fig. 9. Structures of minimum binding energy for *C* (top) and *E* (bottom) conformations of DHN when forming the βCD_2:DHN complexes. HBs shows by dashed lines. Water molecules were removed.

4. Conclusion

Fluorescence measurements reveal that DHN guests form complexes with α- and βCDs with different guest:host stoichiometries, 1:1 and 2:1 respectively. Both 1:1 and 2:1 complex formations are exothermic and they are accompanied by an unfavorable entropy change. Molecular mechanics proves that the formation of such complexes is possible and permits their stoichiometries to be explained. Such stoichiometries are closely related to the length of the DHN guest which can adopt fairly coiled-bulky conformations and the CD sizes. For the hypothetical 1:1 complexes with both CDs a large portion of DHN is outside the cavity. This permits the approximation of a second βCD to the 1:1 βCD:DHN complex up to CD distances where interactions are favorable for the formation of intermolecular HBs between them. This would stabilize the 2:1 stoichiometry complex. This is not probable for the αCD:DHN, as the cavity size does not favor the approximation of a second CD, especially when DHN is in a coiled conformation. The non-bonded van der Waals interactions are mainly responsible for the stability of both 1:1 and 2:1 complexes. Nevertheless electrostatics interactions between CDs also play an important role for this stabilization.

Acknowledgements

This research was supported by MCYT project BQU2001/1158 and GR/MAT/0810/2004. We wish to express our thanks to M.L. Heijnen for assistance with the preparation of the manuscript.

References

[1] J. Szejtli, T. Osa, Comprehensive Supramolecular Chemistry, vol. 3, Cyclodextrins, Elsevier, Oxford, 1996.
[2] V.T. D'Souza, K.B. Lipkowitz, Chem. Rev. 98 (5) (1998) 1741–2076.
[3] A. Harada, Adv. Polym. Sci. 133 (1997) 141–201.
[4] A. Harada, Acc. Chem. Res. 34 (6) (2001) 456–464.
[5] K. Kano, I. Takenoshita, T. Ogawa, Chem. Lett. Chem. Soc. Jpn. (1982) 321–324.
[6] A. Nakajima, Spectrochim. Acta 39A (10) (1983) 913–915.
[7] N. Kobayashi, R. Saito, H. Hino, Y. Hino, A. Ueno, T. Osa, J. Chem. Soc. Perkin. Trans. II (1983) 1031–1035.
[8] S. Hashimoto, J.K. Thomas, J. Am. Chem. Soc. 107 (1985) 4655–4662.
[9] G. Patonay, A. Shapira, P. Diamond, I.M. Warner, J. Phys. Chem. 90 (1986) 1963–1966.
[10] G. Nelson, G. Patonay, I.M. Warner, Appl. Spectrosc. 41 (7) (1987) 1235–1238.
[11] S. Hamai, J. Phys. Chem. 93 (1989) 6527–6529.
[12] G.C. Catena, F. Bright, V. Anal. Chem. 61 (1989) 905–909.
[13] A. Muñoz de la Peña, T.T. Ndou, J.B. Zung, I.M. Warner, J. Phys. Chem. 95 (1991) 3330–3334.
[14] S. Monti, G. Köhler, G. Grabner, J. Phys. Chem. 97 (1993) 13011–13016.
[15] A. Nakamura, S. Sato, K. Hamasaki, A. Ueno, F. Toda, J. Phys. Chem. 99 (1995) 10952–10959.
[16] J.M. Madrid, F. Mendicuti, Appl. Spectrosc. 51 (1997) 1621–1627.
[17] J.M. Madrid, F. Mendicuti, W.L. Mattice, J. Chem. Phys. B 102 (1998) 2037–2044.
[18] J.M. Madrid, M. Villafruela, R. Serrano, F. Mendicuti, J. Phys. Chem. B 103 (1999) 4847–4853.
[19] M. Cervero, F. Mendicuti, J. Phys. Chem. B 104 (2000) 1572–1580.
[20] I. Pastor, A. Di Marino, Mendicuti, J. Phys. Chem. B 106 (2002) 1995–2003.
[21] A. Di Marino, F. Mendicuti, Appl. Spectrosc. 12 (2002) 1579–1587.
[22] M.J. Sherrod, in: J.E.D. Davies (Ed.), Spectroscopic and Computational Studies of Supramolecular Systems, Kluwer Academic Publishers, Dordrecht, The Netherlands, 1992, p. 187.
[23] K.B. Lipkowitz, Chem. Rev. 98 (5) (1998) 1829–1874.
[24] O. Martin, F. Mendicuti, E. Saiz, W.L. Mattice, J. Polym. Sci. Part B: Polym. Phys. Ed. 37 (1999) 253–266.
[25] Sybyl 6.9. Tripos associates, St. Louis, Missouri, USA.
[26] M. Crark, R.C. Cramer III, N. van Opdenbosch, J. Comput. Chem. 10 (1989) 982–1012.
[27] MOPAC-AM1, included in the Sybyl 6.9 package.
[28] W.H. Press, B.P. Flannery, S.A. Teukolski, W.T. Vetterling, Numerical Recipes: The Art of Scientific Computing, Cambridge University Press, 1988, p. 312.
[29] M. Blanco, J. Comput. Chem. 12 (1991) 237–247.
[30] D.V. OĭConnor, W.R. Ware, J.C. André, J. Phys. Chem. 83 (1979) 1333–1343.
[31] J.R. Lakowicz, Principles of Fluorescence Spectroscopy, Kluwer Academic/Plenum Publishers, New York, 1999, p. 129.
[32] MicroCal™ Origin™ 6.0, MicroCal Software Inc. Northampton, MA, USA.
[33] M.V. Rekharsky, Y. Inoue, Chem. Rev. 98 (5) (1998) 1875–1917.